Fabrication of Flexible MoS_2 Thin-Film Transistor Arrays for Practical Gas-Sensing Applications

*Qiyuan He, Zhiyuan Zeng, Zongyou Yin, Hai Li, Shixin Wu, Xiao Huang, and Hua Zhang**

By combining two kinds of solution-processable two-dimensional materials, a flexible transistor array is fabricated in which MoS_2 thin film is used as the active channel and reduced graphene oxide (rGO) film is used as the drain and source electrodes. The simple device configuration and the 1.5 mm-long MoS_2 channel ensure highly reproducible device fabrication and operation. This flexible transistor array can be used as a highly sensitive gas sensor with excellent reproducibility. Compared to using rGO thin film as the active channel, this new gas sensor exhibits much higher sensitivity. Moreover, functionalization of the MoS_2 thin film with Pt nanoparticles further increases the sensitivity by up to ~3 times. The successful incorporation of a MoS_2 thin-film into the electronic sensor promises its potential application in various electronic devices.

1. Introduction

Electronic sensors based on the field-effect transistor (FET)[1–3] offer a simple, efficient, and low-cost sensing platform for various chemical and biological detections. The recent development of active channels with nanostructured semiconductors has greatly enriched the capabilities of FET-based electronic sensors, which exhibit the significantly improved sensitivity. One-dimensional (1D) silicon nanowires[1,4] and carbon nanotube (CNT),[5–7] and two-dimensional (2D) graphene[8–12] and its derivatives[14–16] are among the most promising channel materials in electronic sensors. In particular, graphene-based electronic sensors have been extensively studied in the past few years.[13–18] For example, the FET sensor based on the mechanically cleaved single-layer graphene showed an ultimate sensitivity, *i.e.* the single gas molecule was detected.[18] However, the practical electronic sensors require the low-cost, massive production of active channels with reliable and reproducible sensing performance. Therefore, the scalable production of graphene by chemical vapor deposition (CVD)[19–22] or chemical synthesis of reduced graphene oxide (rGO)[8,13–16,23,24] has attracted much interest. Importantly, the emergence of rGO, one kind of solution-processable graphene derivative, has boosted the studies on graphene-based thin-film transistor (TFT),[13,15,23] since it is compatible with the conventional thin-film technologies such as spin-coating[24] and inkjet-printing.[25] Therefore, the flexibility, robustness and reproducibility of rGO-based thin-film device makes it a promising candidate for the practical electronic sensor. However, graphene without proper surface functionalization[26,27,28] is a semi-metal[29,30] with a zero bandgap, thus resulting in the weak switching property.

Recent studies on layer-structured transition-metal dichalocogenides opened a new avenue for the fabrication of electronic devices based on a series of novel 2D semiconducting materials.[31–42] For example, single-layer MoS_2 nanosheets obtained from the mechanical cleavage exhibited outstanding performance in a top-gate FET with ON/OFF ratio exceeding 10^8.[33] In addition, our group has fabricated a phototransistor based on the single-layer MoS_2, which exhibited the superior photoresponsivity compared to a device made from the single-layer graphene.[41] Moreover, we reported the electronic sensors based on the mechanically exfoliated single- to four-layer MoS_2 nanosheets, which

Q. He, Z. Zeng, Dr. Z. Yin, Dr. H. Li, Dr. S. Wu, Dr. X. Huang, Prof. H. Zhang
School of Materials Science and Engineering
Nanyang Technological University
50 Nanyang Avenue, Singapore 639798, Singapore
Tel: (+65) 67905175; Fax: (+ 65) 67909081
Website: http://www.ntu.edu.sg/home/hzhang
E-mail: hzhang@ntu.edu.sg

DOI: 10.1002/smll.201201224

NANO MICRO small

showed extremely high sensitivity for toxic gas detection (80% decrease of channel conductance upon exposure to the 2 ppm NO).[42] However, similar to graphene, the practical application based on such 2D semiconducting materials also requires the facile procedures for low-cost and high-yield preparation of the materials. Recently, ultrasonication of bulk layered materials in strong polar solvents, which was previously used to prepare graphene suspension, was used to produce a series of single to few-layer materials including MoS_2, WS_2, $MoSe_2$, etc.[35] However, it is difficult to control the resulting materials in shape, lateral size, thickness and layer numbers. Alternatively, by using a controllable lithiation process, our group has successfully fabricated 2D nanosheets (MoS_2, WS_2, TiS_2, TaS_2 and ZrS_2) with the high yield of single layers.[37a] Thus obtained 2D materials are stable in many solvents, providing the solution-processability for their various applications.

In this communication, we present the fabrication of a flexible TFT array based on the MoS_2 thin film and then demonstrate its application in toxic gas detection. A patterned rGO film on polyethylene terephthalate (PET) substrate was used as an array of drain and source electrodes. The MoS_2 thin film was then deposited on the rGO electrodes by spin-coating of a suspension of single-layer MoS_2 sheets. The MoS_2 thin film showed the comparable flexibility to graphene thin film, which is commonly used in the flexible electronics. By combining the MoS_2 channel with the rGO electrodes, the TFT sensor array exhibited high flexibility, which could survive over 5000 bending cycles without losing its excellent sensing performance. The MoS_2 sensor showed a better performance in the detection of NO_2, compared to the similar device based on the rGO thin film. Functionalization of the MoS_2 thin film with Pt nanoparticles (PtNPs) further increased the sensitivity of the TFT sensor by ~3 times. Importantly, the simple thin-film configuration of our sensor array not only allows the facile fabrication and operation procedures, but also ensures the high reproducibility of sensing performance of different devices, which could have great practical applications in electronic devices.

2. Results and Discussion

The fabrication process of the MoS_2 TFT array is illustrated in **Scheme 1** and described in the experimental section. Briefly, a uniform GO film was first spin-coated on a flexible PET substrate. The GO line patterns were then generated by the "scratch method" developed by our group.[43] The patterned line width and the space between the adjoining GO lines were 2 mm and 1.5 mm, respectively. The GO patterns were reduced by hydrazine vapor to obtain the conductive rGO patterns which were then used as drain and source electrodes. The thickness of the rGO film was ~10 nm, confirmed by atomic force microscopy (AFM) (Figure S1a in Supporting Information, SI). Our previous studies suggested that the 10 nm-thick rGO thin film, with the weak switching behavior but good electrical conductivity, is a promising flexible electrodes.[15] Then a continuous MoS_2 thin film was spin-coated on top of the rGO patterns and used as the active channel for the obtained TFT array. Here, the MoS_2 aqueous solution, containing the single-layer MoS_2 sheets with the size of ca. 0.5 to 2 μm (Figure S2 in SI), was prepared from the electrochemical lithiation and sonication followed by the centrifugation-assisted separation process.[14,37] It is crucial to produce such high-quality MoS_2 dispersion for fabrication of a uniform MoS_2 thin film. As a control experiment, devices with 4 nm thick rGO thin film (Figure S1b in SI) as the active channel were fabricated by using the similar process as mentioned above for fabrication of the MoS_2-based devices. Note that the previous studies usually focused on the miniaturization of electronic sensors, where the short channels of less than 10 μm were typically employed.[17,18] Unfortunately, these short channels were fragile and subjected to the damage during the fabrication and/or repeated operation of sensors, resulting in poor reproducibility.[17,44] To overcome this problem, the width of MoS_2 channel in the presence work was fixed at 1.5 mm, determined by the space between the rGO electrodes. This relatively long channel ensures a high device robustness and facile device operation. Finally, a drop of silver paint was deposited on one end of each rGO line patterns. The silver pads were used for the attachment of probes to enhance the robustness of the rGO electrodes during the multiple electronic tests. As shown in Scheme 1, a typical sensing array with six operational sensors were obtained.

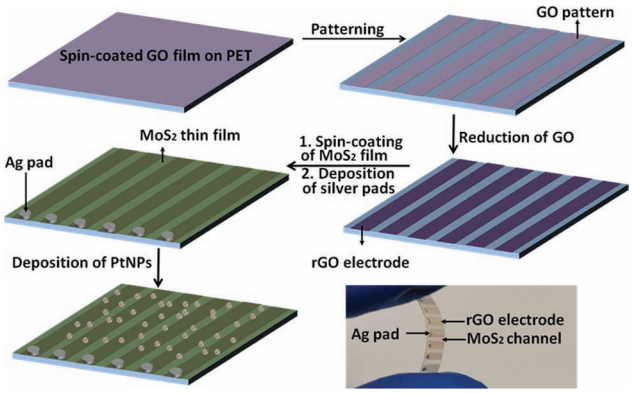

Scheme 1. Schematic illustration of the fabrication process of MoS_2 TFT array on PET substrate and a photograph of the TFT sensor array.

Although the bulk MoS_2 is an n-type semiconductor,[33] our MoS_2 TFTs showed a weak p-type behavior in a typical back-gate field-effect measurement (Figure S3a in SI). Similar weak p-type behavior after lithiation was also observed in the previous study of a back-gate FET based on the individual single-layer MoS_2 sheet.[37a] Such change of semiconducting property arises from the structural change after the lithium intercalation process.[45,46] The low ON/OFF characteristic (Figure S3a in SI) can be explained by the thin film morphology containing numerous sheet junctions, which lowered the carrier mobility and hence compromised the field effect of the devices. It is worth metioning that although the ON/OFF ratio above 2 is typically observed in FET based on single-layer graphene or rGO sheet,[12,13] the rGO thin film transistors showed no obvious switching behavior in the back-gate measurement (Figure S3b in SI). The observable switching behavior of MoS_2 thin film suggests that MoS_2 could be a better choice for the channel material in electronic sensors. In addition, compared to the back-gate measurement operated on 600 nm SiO_2, the switching behavior of MoS_2

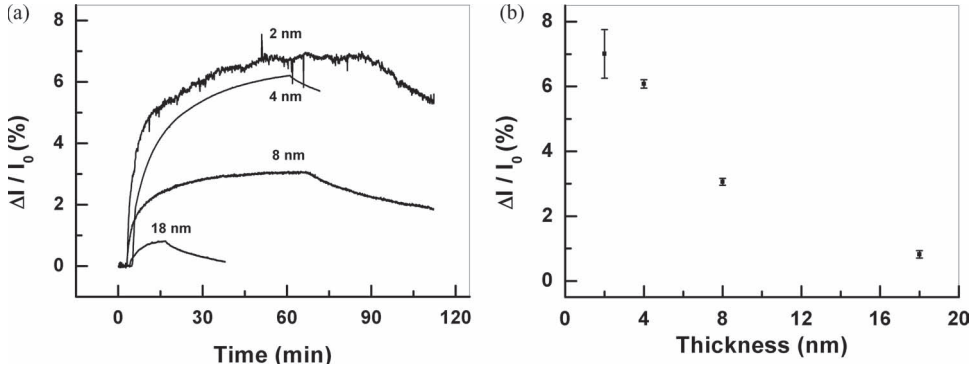

Figure 1. (a) Detection of 1.2 ppm NO_2 using MoS_2 TFT sensors on PET with different thickness of MoS_2 thin film. (b) The plot of the detection sensitivity of 1.2 ppm NO_2 versus the thickness of MoS_2 film. Standard error was obtained by measuring 3 devices.

TFT can be clearly observed in a typical solution-gate setup with an ON/OFF ratio of ~10 (Figure S4 in SI).

As a proof of concept, the fabricated MoS_2 sensing array was used to detect NO_2, a prominent air pollutant. In order to optimize the sensitivity of the MoS_2-based gas sensor, the MoS_2 channels with different thicknesses were fabricated. The thickness of MoS_2 thin film can be controlled by the volume of MoS_2 solution used in the spin-coating process. Four TFT devices with different thickness of MoS_2 as channel were fabricated, as confirmed by the AFM measurements (Figure S5 in SI). As shown in **Figure 1**a, the conductance of the MoS_2 channel increased upon adsorption of NO_2 molecules. Previous studies suggested that the contact resistance between semiconducting channel and metal electrodes has an observable[47] and sometimes dominant effect[48] on the device performance. However, since the MoS_2 channel used here is relatively long, ~1.5 mm, the overall resistance of the device is dominated by the intrinsic resistance of the MoS_2 film, instead of the contact resistance between the MoS_2 channel and the rGO electrodes. Furthermore, the previously reported two-step current response in electronic sensors based on the mechanically exfoliated MoS_2 sheets was not observed in the present MoS_2 TFTs. This suggests a different surface chemistry between the MoS_2 nanosheets prepared from the electrochemical lithiation[37a] and those from the mechanical exfoliation.[42] Therefore, we believe the sensing mechanism in our study originates from the direct charge transfer from electron-withdrawing NO_2 molecules adsorped on the MoS_2 film, resulting in the increase of conductance in p-type transistors.[13,26,49,50] In a control experiment as shown in Figure S6 in SI, the MoS_2 device showed a negative response to the exposure of 0.2 ppm H_2S due to its electron-donating property.

Figure 1b shows the dependence of device sensitivity towards the NO_2 detection on the thickness of MoS_2 film. Here, the sensitivity was defined as $(I_1–I_0)/I_0 \times 100\%$, where I_0 is the initial stable current of the device and I_1 is the stable current after the device exposure to 1.2 ppm NO_2. The sensitivity of MoS_2 TFT decreased dramatically with the thickness increase of MoS_2 film, from ~7.0% at thickness of 2.0 nm to ~0.8% at thickness of 18 nm (Figure 1b). This is because the thickness increase of MoS_2 film lowers the surface area-to-volume ratio of the MoS_2 channel, resulting in the decrease of gas sensitivity. However, the device current became unstable at a thickness below 4 nm (see the curve of 2 nm-thick MoS_2 film in Figure 1a), which might arise from the discontinuous MoS_2 film (see AFM image in Figure S5a in SI). Therefore, in the following experiments, the optimized thickness (4 nm) of MoS_2 channel (see Figure S5b in SI) with a corresponding sensitivity of ~6.1% was used.

In a control experiment, a rGO-based TFT on PET with 4 nm-thick rGO thin film (see AFM image in Figure S1b in SI) as the active channel was also used to detect the 1.2 ppm NO_2 (**Figure 2**a). The gas sensitivity (~3.4% at 1.2 ppm) of the rGO-based TFT is lower than that obtained from both

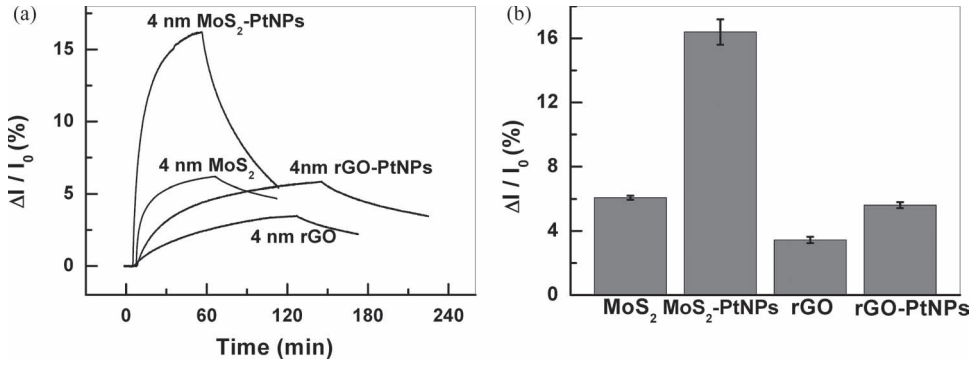

Figure 2. (a) Typical current response of TFT sensor on PET upon exposure of 1.2 ppm NO_2 with channel of rGO, rGO-PtNPs, MoS_2 and MoS_2-PtNPs, respectively. (b) The current change of TFT sensor on PET with channel of rGO, rGO-PtNPs, MoS_2 and MoS_2-PtNPs, respectively. Standard error was obtained by measuring 3 devices.

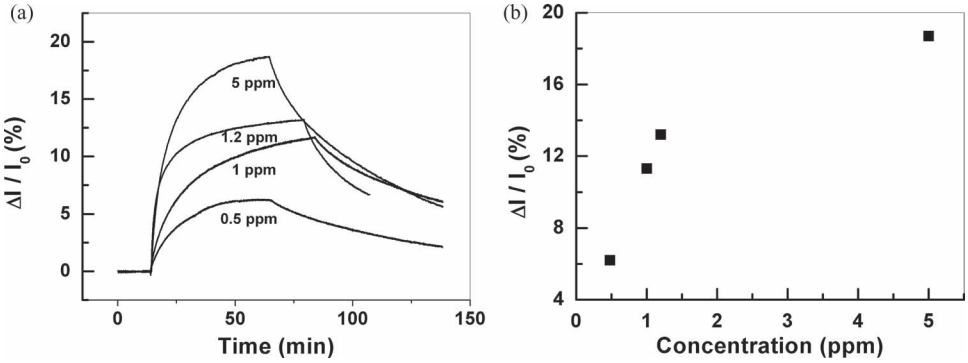

Figure 3. (a) Typical current response of one MoS_2-PtNPs-based sensor upon exposure of different concentration of NO_2. (b) The percent current change versus the concentration of NO_2.

the MoS_2 TFT (sensitivity of ~6.1% at 1.2 ppm) (Figure 2a) and the FET sensor based on the single-layer MoS_2.[42] The better performance of the MoS_2-based electronic sensor can be attributed to the better switching behavior of MoS_2 TFT compared to the rGO TFT (Figure S3 in SI). Despite the excellent sensitivity of our MoS_2-based gas sensor, the response and recovery time is still relatively long (>30 min). This disadvantage can be overcome by operating the device at a higher temperature.[24]

Moreover, the MoS_2 sensor array on PET shows excellent flexibility. As shown in Figure S7 in SI, the device did not lose any conductance after 5000 bending cycles (bent radius of 4 mm). Note that there was an increase of the channel resistance during the initial 10 bending cycles, which might arise from the rearrangement of the stacked MoS_2 sheets. Our experimental result shows that the sensor array could function well in the gas detection even after 5000 bending cycles, making MoS_2-based devices among the best flexible electronic devices, even comparable with the full-rGO[15] and CVD-graphene devices.[51]

The previous studies have suggested that the proper functionalizaion of semiconducting channel may greatly enhance the gas sensitivity of electronic sensors.[47,52–58] For example, the sensor based on the rGO-Pd nanoparticles (rGO-PdNPs) hybrid channel gave 2 times better sensitivity in the NO detection than that based on the pure rGO channel.[47] The electronic sensor based on the In_2O_3 nanowires (In_2O_3NWs) functionalized with Au nanoparticles (AuNPs) gave more than 30 times of sensitivity in the CO detection than that based on the pure In_2O_3NWs.[56] Here, in order to increase the sensitivity of gas sensors, we functionalized the MoS_2 thin film with PtNPs, referred to as MoS_2-PtNPs. The thickness of the MoS_2 thin film was 4 nm. PtNPs were directly deposited on the MoS_2 film by a photoreduction method, as described in the experimental section. Scanning electron microscopy (SEM) and energy-dispersive X-ray spectroscopy (EDX) confirmed the presence of PtNPs (Figure S8 in SI). As shown in AFM images in Figure S9a in SI, the PtNPs with diameter of 5.7 ± 1.6 nm were deposited on the MoS_2 film. The density of PtNPs was carefully controlled to avoid the fuse of PtNPs. Note that if the fused-PtNPs functionalized MoS_2 film (Figure S10a in SI) was used as channel, the fabricated TFT showed the dramatic increase of the conductance, which led to the loss of the sensing capability (Figure S10b in SI).

As shown in Figure 2, the incorporation of PtNPs (Figure S9 in SI) further increased the sensitivity of the MoS_2 TFT by ~3 times.The reason for such increase in sensitivity is still under debate. Li *et al.* suggested that the formation of a Schottky junction between the p-type semiconducting channel and metal nanoparticles was responsible for the improved sensitivity.[47] It could also be explained by the enhanced adsorption[52–54] of gas molecules at the interface of nanoparticles and semiconducting channel. Here, a control experiment was carried out on the rGO-PtNPs, in which the diameter of PtNPs is 6.6 ± 1.3 nm (Figure S9b in SI). The experimental result showed that only a small enhancement (<30%) in sensitivity was observed as compared to the bare rGO device (Figure 2). The greater enhancement in sensing performance of MoS_2-PtNPs-based device compared to rGO-PtNPs-based device suggested that the PtNP-modified sensor is not same as the Pd nanoparticle (PdNP)-functionalized gas sensor,[52,53] in which the enhancement of gas sensitivity was attributed to the enhanced gas adsorption on the surface of PdNPs. Hence, the sensitivity increase in our device is more likely due to the change of the Schottky barrier between the PtNPs and the semiconducting MoS_2 channel upon the gas adsorption.[47,55,56,59] However, the detailed mechanism needs the further investigation.

Figure 3a shows a typical current response of an MoS_2-PtNPs-based device to the different concentration of NO_2. Because of the safety concern, the highest concentration tested here was 5 ppm. The device is allowed to return to its initial current (fully desorption of the adsorbed NO_2) before it was used for another detection. As shown in Figure 3b, a nonlinear relation between gas sensitivity and the NO_2 concentration was found, suggesting that the linear range of the MoS_2 sensor was below 1.5 ppm. The detection limit of the MoS_2-PtNPs device towards NO_2 was calculated to be 2 ppb based on a signal-to-noise ratio of 3. This detection limit is better than the most nanowire[60] and nanotube[61] based gas sensors.

3. Conclusion

In conclusion, we have reported a fully solution-processed fabrication of flexible thin-film transistor (TFT) array based on the MoS_2 thin film channel and rGO electrodes. The

obtained device shows high flexibility and excellent reproducibility from batch to batch. The TFT array is used as high-performance, easy-operable and robust gas sensors for the NO_2 detection. Superior sensitivity of the MoS_2-based device, compared to the rGO thin film-based device, is observed. Functionalization of the MoS_2 thin film with Pt nanoparticles can further increase the sensitivity by ~3 times. A calculated detection limit of 2 ppb is achieved by using the MoS_2-PtNPs as channel. Our study suggests that the high-quality and solution-processable single-layer MoS_2 is a promising channel material used for the practical electronic sensors.

4. Experimental Section

Fabrication of MoS_2 Thin Film Transistor (TFT): Intercalation and exfoliation of MoS_2 was carried out using our recently developed method.[37a] Graphene oxide (GO) was synthesized from the microwave-expanded graphite by the modified Hummers method.[62,63]Scheme 1 shows how to fabricate the MoS_2 TFT array on PET. GO film was obtained by spin-coating a GO methanol suspension (1.5 mg/mL) on a 2.2 cm × 2.2 cm PET film. Our previously developed "scratch method" was used to create GO line patterns with 2 mm width and 1.5 mm interdistance between two adjoining GO lines.[15,43] The GO patterns were then reduced by hydrazine vapor to obtain the conductive rGO patterns used for the source and drain electrodes. The thickness of the rGO film was controlled by the volume of GO methanol suspension (1.5 mg/mL) used in spin-coating process. A MoS_2 methanol solution was purified by centrifugation to get the single-layer MoS_2 sheets with the size of ca. 0.5 to 2 μm (Figure S2 in SI). The MoS_2 thin film was obtained by spin-coating the aforementioned MoS_2 methanol suspension on the PET substrate. Silver paint was then deposited at one end of each rGO line pattern. The obtained silver pads were used for the attachment of probes to enhance the robustness of the rGO electrodes during the electronic tests. The device was then annealed at in a vacuum oven at 50 °C overnight. Finally, the PET film (2.2 cm × 2.2 cm) was cut to 2.2 cm × 3 mm, as shown in the photo in Scheme 1. Therefore, the length and width of the MoS_2 channel were 1.5 and 3 mm, respectively.

Functionalization and Characterization of MoS_2 or rGO Channel with Pt Nanoparticles (PtNPs): PtNPs were deposited on the surface of MoS_2 film by the photoreduction method. The MoS_2 thin film on PET was immersed in an aqueous solution of 0.2 mM K_2PtCl_4 and 0.3 mM sodium citrate prepared in a 10 mL glass vial and then irradiated with a 150 W halogen lamp at 30% of its full intensity for 12 h.[12] After the reaction, the MoS_2 film was rinsed with ethanol and DI-water and then dried with N_2. The same method was used to functionalize rGO with PtNPs. Atomic force microscopy (AFM, Dimension 3100 with Nanoscope IIIa controller, Veeco, CA, USA) images were taken in tapping mode in air. SEM images were obtained by the field emission scanning electron microscopy (FESEM, Model JSM-7600F, JEOL Ltd., Tokyo).

Electrical Measurements: All the electrical measurements were carried out on a Keithley 4200 semiconductor characterization system at ambient conditions. The back-gate field-effect test of pure MoS_2 and rGO channel was conducted on Si/SiO_2 (600 nm) substrate using the thermally evaporated 5 nm thick Cr/50 nm thick Au as drain and source electrodes. The length and width of the channel were 3 mm and 500 μm, respectively. The solution-gate experiments were carried out accroding to literatures[14,15] with channel length of 3 mm in 1× PBS buffer. The bending test of MoS_2 TFT on PET was carried out by measuring the device conductance (I_{ds}) at V_{ds} = 0.5 V after certain bending cycles. Note that all sensing experiments are based on devices fabricated on PET substrates. Devices fabricated on SiO_2 substrates are only for AFM and SEM characterization, and the back-gate field-effect tests.

Gas Sensing: The as-prepared TFT devices were located in the chamber of a homemade sensing system in a glove box. The Keithley 4200 semiconductor characterization system was used to monitor the real-time current change using the two-point measurement in a glove box. The concentration of NO_2 was controlled by a mixture of NO_2 (5.1 ppm in N_2) and N_2 (99.999%) flow (National Oxygen Pte Ltd, Singapore) measured by the flow meters.

Supporting Information

Supporting Information is available from the Wiley Online Library or from the author.

Acknowledgements

Q.H. and Z.Z. contributed equally to this work. This work was supported by MOE under AcRF Tier 2 (ARC 10/10, No. MOE2010-T2-1-060), Singapore National Research Foundation under CREATE programme: Nanomaterials for Energy and Water Management, and NTU under the SUG (M4080865.070.706022) in Singapore.

[1] F. Patolsky, G. F. Zheng, C. M. Lieber, *Anal. Chem.* **2006**, *78*, 4260.
[2] Y. L. Guo, G. Yu, Y. Q. Liu, *Adv. Mater.* **2010**, *22*, 4427.
[3] P. A. Hu, J. Zhang, L. Li, Z. L. Wang, W. O'Neill, P. Estrela, *Sensors* **2010**, *10*, 5133.
[4] F. Patolsky, B. P. Timko, G. F. Zheng, C. M. Lieber, *MRS Bull.* **2007**, *32*, 142.
[5] Q. Cao, J. A. Rogers, *Adv. Mater.* **2009**, *21*, 29.
[6] P. Bondavalli, P. Legagneux, D. Pribat, *Sens. Actuator B-Chem.* **2009**, *140*, 304.
[7] B. L. Allen, P. D. Kichambare, A. Star, *Adv. Mater.* **2007**, *19*, 1439.
[8] X. Huang, Z. Y. Yin, S. X. Wu, X. Y. Qi, Q. Y. He, Q. C. Zhang, Q. Y. Yan, F. Boey, H. Zhang, *Small* **2011**, *7*, 1876.
[9] Y. Liu, X. Dong, P. Chen, *Chem. Soc. Rev.* **2012**, *41*, 2283.
[10] H. J. Jiang, *Small* **2011**, *7*, 2413.
[11] F. Chen, Q. Qing, J. L. Xia, N. J. Tao, *Chem. Asian J.* **2010**, *5*, 2144.
[12] X. Huang, X. Qi, F. Boey, H. Zhang, *Chem. Soc. Rev.* **2012**, *41*, 666.
[13] Q. He, S. X. Wu, Z. Y. Yin, H. Zhang, *Chem. Sci.* **2012**, *3*, 1764.
[14] Q. He, H. G. Sudibya, Z. Yin, S. Wu, H. Li, F. Boey, W. Huang, P. Chen, H. Zhang, *ACS Nano* **2010**, *4*, 3201.
[15] Q. He, S. Wu, S. Gao, X. Cao, Z. Yin, H. Li, P. Chen, H. Zhang, *ACS Nano* **2011**, *5*, 5038.
[16] H. G. Sudibya, Q. He, H. Zhang, P. Chen, *ACS Nano* **2011**, *5*, 1990.
[17] Y. Ohno, K. Maehashi, Y. Yamashiro, K. Matsumoto, *Nano Lett.* **2009**, *9*, 3318.
[18] F. Schedin, A. K. Geim, S. V. Morozov, E. W. Hill, P. Blake, M. I. Katsnelson, K. S. Novoselov, *Nat. Mater.* **2007**, *6*, 652.

[19] X. Li, W. Cai, J. An, S. Kim, J. Nah, D. Yang, R. Piner, A. Velamakanni, I. Jung, E. Tutuc, S. K. Banerjee, L. Colombo, R. S. Ruoff, *Science* **2009**, *324*, 1312.
[20] X. Dong, Y. Shi, W. Huang, P. Chen, L. J. Li, *Adv. Mater.* **2010**, *22*, 1649.
[21] X. H. Cao, Y. M. Shi, W. H. Shi, G. Lu, X. Huang, Q. Y. Yan, Q. C. Zhang, H. Zhang, *Small* **2011**, *7*, 3163.
[22] Y. Huang, X. Dong, Y. Liu, L.-J. Li, P. Chen, *J. Mater. Chem.* **2011**, *21*, 12358.
[23] J. T. Robinson, F. K. Perkins, E. S. Snow, Z. Wei, P. E. Sheehan, *Nano Lett.* **2008**, *8*, 3137.
[24] J. D. Fowler, M. J. Allen, V. C. Tung, Y. Yang, R. B. Kaner, B. H. Weiller, *ACS Nano* **2009**, *3*, 301.
[25] V. Dua, S. P. Surwade, S. Ammu, S. R. Agnihotra, S. Jain, K. E. Roberts, S. Park, R. S. Ruoff, S. K. Manohar, *Angew. Chem. Int. Ed.* **2010**, *49*, 2154.
[26] J. Berashevich, T. Chakraborty, *Phys. Rev. B* **2010**, *81*, 205431.
[27] X. Wang, Y. Ouyang, L. Jiao, H. Wang, L. Xie, J. Wu, J. Guo, H. Dai, *Nat. Nanotechnol.* **2011**, *6*, 563.
[28] R. Balog, B. Jorgensen, L. Nilsson, M. Andersen, E. Rienks, M. Bianchi, M. Fanetti, E. Laegsgaard, A. Baraldi, S. Lizzit, Z. Sljivancanin, F. Besenbacher, B. Hammer, T. G. Pedersen, P. Hofmann, L. Hornekaer, *Nat. Mater.* **2010**, *9*, 315.
[29] A. K. Geim, K. S. Novoselov, *Nat. Mater.* **2007**, *6*, 183.
[30] I. Meric, M. Y. Han, A. F. Young, B. Ozyilmaz, P. Kim, K. L. Shepard, *Nat. Nanotechnol.* **2008**, *3*, 654.
[31] K. S. Novoselov, D. Jiang, F. Schedin, T. J. Booth, V. V. Khotkevich, S. V. Morozov, A. K. Geim, *Proc. Natl. Acad. Sci. USA* **2005**, *102*, 10451.
[32] a) A. Castellanos-Gomez, N. Agrait, G. Rubio-Bollinger, *Appl. Phys. Lett.* **2010**, *96*; b) S. Cho, N. P. Butch, J. Paglione, M. S. Fuhrer, *Nano Lett.* **2011**, *11*, 1925.
[33] B. Radisavljevic, A. Radenovic, J. Brivio, V. Giacometti, A. Kis, *Nat. Nanotechnol.* **2011**, *6*, 147.
[34] S. Cho, N. P. Butch, J. Paglione, M. S. Fuhrer, *Nano Lett.* **2011**, *11*, 1925.
[35] J. N. Coleman, M. Lotya, A. O'Neill, S. D. Bergin, P. J. King, U. Khan, K. Young, A. Gaucher, S. De, R. J. Smith, I. V. Shvets, S. K. Arora, G. Stanton, H.-Y. Kim, K. Lee, G. T. Kim, G. S. Duesberg, T. Hallam, J. J. Boland, J. J. Wang, J. F. Donegan, J. C. Grunlan, G. Moriarty, A. Shmeliov, R. J. Nicholls, J. M. Perkins, E. M. Grieveson, K. Theuwissen, D. W. McComb, P. D. Nellist, V. Nicolosi, *Science* **2011**, *331*, 568.
[36] A. Splendiani, L. Sun, Y. Zhang, T. Li, J. Kim, C.-Y. Chim, G. Galli, F. Wang, *Nano Lett.* **2010**, *10*, 1271.
[37] a) Z. Zeng, Z. Yin, X. Huang, H. Li, Q. He, G. Lu, F. Boey, H. Zhang, *Angew. Chem. Int. Ed.* **2011**, *50*, 11093; b) Z. Y. Zeng, T. Sun, J. X. Zhu, X. Huang, Z. Y. Yin, G. Lu, Z. X. Fan, Q. Y. Yan, H. H. Hng, H. Zhang, *Angew. Chem. Int. Ed.* **2012**, DOI: 10.1002/anie.201204208; c) J. Q. Liu, Z. Y. Zeng, X. H. Cao, G. Lu, L. H. Wang, Q. L. Fan, W. Huang, H. Zhang, *Small* **2012**, DOI: 10.1002/smll.201200999.
[38] C. Lee, Q. Li, W. Kalb, X.-Z. Liu, H. Berger, R. W. Carpick, J. Hone, *Science* **2010**, *328*, 76.
[39] C. Lee, H. Yan, L. E. Brus, T. F. Heinz, J. Hone, S. Ryu, *ACS Nano* **2010**, *4*, 2695.
[40] Z. Cheng, Q. Li, Z. Li, Q. Zhou, Y. Fang, *Nano Lett.* **2010**, *10*, 1864.
[41] Z. Yin, H. Li, H. Li, L. Jiang, Y. Shi, Y. Sun, G. Lu, Q. Zhang, X. Chen, H. Zhang, *ACS Nano* **2012**, *6*, 74.
[42] H. Li, Z. Yin, Q. He, H. Li, X. Huang, G. Lu, D. W. H. Fam, A. I. Y. Tok, Q. Zhang, H. Zhang, *Small* **2012**, *8*, 63.
[43] B. Li, X. Cao, H. G. Ong, J. W. Cheah, X. Zhou, Z. Yin, H. Li, J. Wang, F. Boey, W. Huang, H. Zhang, *Adv. Mater.* **2010**, *22*, 3058.
[44] G. Lu, S. Park, K. Yu, R. S. Ruoff, L. E. Ocola, D. Rosenmann, J. Chen, *ACS Nano* **2011**, *5*, 1154.
[45] G. Eda, H. Yamaguchi, D. Voiry, T. Fujita, M. Chen, M. Chhowalla, *Nano Lett.* **2011**, *11*, 5111.
[46] J. Heising, M. G. Kanatzidis, *J. Am. Chem. Soc.* **1999**, *121*, 11720.
[47] W. Li, X. Geng, Y. Guo, J. Rong, Y. Gong, L. Wu, X. Zhang, P. Li, J. Xu, G. Cheng, M. Sun, L. Liu, *ACS Nano* **2011**, *5*, 6955.
[48] N. Peng, Q. Zhang, C. L. Chow, O. K. Tan, N Marzari, *Nano Lett.* **2009**, *9*, 1626.
[49] T. O. Wehling, K. S. Novoselov, S. V. Morozov, E. E. Vdovin, M. I. Katsnelson, A. K. Geim, A. I. Lichtenstein, *Nano Lett.* **2007**, *8*, 173.
[50] L. Valentini, I. Armentano, J. M. Kenny, C. Cantalini, L. Lozzi, S. Santucci, *Appl. Phys. Lett.* **2003**, *82*, 961.
[51] L. Gomez De Arco, Y. Zhang, C. W. Schlenker, K. Ryu, M. E. Thompson, C. Zhou, *ACS Nano* **2010**, *4*, 2865.
[52] A. Kolmakov, D. O. Klenov, Y. Lilach, S. Stemmer, M. Moskovits, *Nano Lett.* **2005**, *5*, 667.
[53] J. L. Johnson, A. Behnam, S. J. Pearton, A. Ural, *Adv. Mater.* **2010**, *22*, 4877.
[54] G. Lu, L. E. Ocola, J. Chen, *Adv. Mater.* **2009**, *21*, 2487.
[55] X. H. Chen, M. Moskovits, *Nano Lett.* **2007**, *7*, 807.
[56] N. Singh, R. K. Gupta, P. S. Lee, *ACS Appl. Mater. Interfaces* **2011**, *3*, 2246.
[57] H. Chang, Z. H. Sun, K. Y. Ho, X. M. Tao, F. Yan, W. M. Kwok, Z. J. Zheng, *Nanoscale* **2011**, *3*, 258.
[58] H. Chang, Z. H. Sun, Q. H. Yuan, F. Ding, X. M. Tao, F. Yan, Z. J. Zheng, *Adv. Mater.* **2010**, *22*, 4872.
[59] T. Y. Wei, P. H. Yeh, S. Y. Lu, Z. L. Wang, *J. Am. Chem. Soc.* **2009**, *131*, 17690.
[60] N. S. Ramgir, Y. Yang, M. Zacharias, *Small* **2010**, *6*, 1705.
[61] T. Zhang, S. Mubeen, N. V Myungl, M. A. Deshusses1, *Nanotechnology* **2008**, *19*, 332001.
[62] X. Z. Zhou, X. Huang, X. Y. Qi, S. X. Wu, C. Xue, F. Y. C. Boey, Q. Y. Yan, P. Chen, H. Zhang, *J. Phys. Chem. C* **2009**, *113*, 10842.
[63] D. Li, M. B. Muller, S. Gilje, R. B. Kaner, G. G. Wallace, *Nat. Nanotechnol.* **2008**, *3*, 101.

Received: June 2, 2012
Published online: July 7, 2012